Pumping in vertical and horizontal target configurations on JET in L-mode; an interpretive study using EDGE2D-EIRENE

D. Moulton[1,2], M. Groth[2], D. Harting[1], S. Wiesen[3], S. Varoutis[4], C. Gleason-González[4] and JET Contributors*

*EUROfusion Consortium, JET, Culham Science Centre, Abingdon, OX14 3DB, UK; [1]CCFE, Culham Science Centre, Abingdon, Oxon, OX14 3DB, UK; [2]Aalto University, Association EURATOM-Tekes, Espoo, Finland; [3]Forschungszentrum Jülich GmbH, Institut für Energie- und Klimaforschung - Plasmaphysik, 52425 Jülich, Germany; [4]Karlsruhe Institute of Technology, Institute for Technical Physics, 76344 Karlsruhe, Germany; *See the Appendix of F. Romanelli et al., Proceedings of the 25th IAEA Fusion Energy Conference 2014, Saint Petersburg, Russia*

Introduction

Multifluid edge codes such as SOLPS have been used to predict the pumped flux on ITER [1]. However, calculated pumped fluxes have rarely been validated against current experiments. On JET, this has been due to the lack of a sub-divertor model in the in-house multifluid edge code EDGE2D-EIRENE [2, 3, 4]. In this paper we present such a model, and benchmark it against experiments in vertical target (VT) and horizontal target (HT) configurations. The experiment modelled here has been described previously in [5]. L-mode density scans were carried out in VT and HT configurations, with $I_p = 2.5$ MA, $B_T = 2.5$ T, $P_{in} = 3$ MW. The simulations presented here are based on those discussed in [5] but with a sub-divertor model included.

The EDGE2D-EIRENE sub-divertor module

Figure 1a shows the geometry used in the simulations. Outlines of the EDGE2D (plasma-solving) grids are shown for the HT (red) and VT (blue) configurations. With the new sub-divertor module included in the code, the EIRENE (neutral-solving) grid now spans the entire sub-divertor domain. The location of the baratron pressure gauge, used to measure the experimental sub-divertor pressure p_{subdiv}, lies inside the simulation domain, as shown by the red asterisk. The simulation puff was placed at the inner divertor base, as was predominantly the case in experiment. At this stage we have assumed the sub-divertor geometry to be toroidally symmetric. The simulated sub-divertor walls were set to 300°C everywhere except for the radiation baffles, poloidal field coils and baratron pipe, which were set to 20°C. Neutral-neutral collisions were not simulated. We assume here that deuterium retention and/or outgassing by the ITER-like wall in L-mode is negligible compared to the D_2 puff rate Φ_{puff} [6]. In the steady state, it follows that the pumped D_2 flux is equal to the puff: $\Phi_{pump} = \Phi_{puff}$.

Figure 1b shows an example of the simulated D_2 density near the cryopump, with the radiation-blocking baffles included. In the absence of neutral-neutral collisions, the density at any point is set by the number of straight-line neutral trajectories passing through that point. Thus, the density drops beyond the divertor throat baffle (which blocks neutrals coming from their source in the divertor), and also towards the upper portion of the cryopump surface, where neutral trajectories are no longer received directly from the throat baffle.

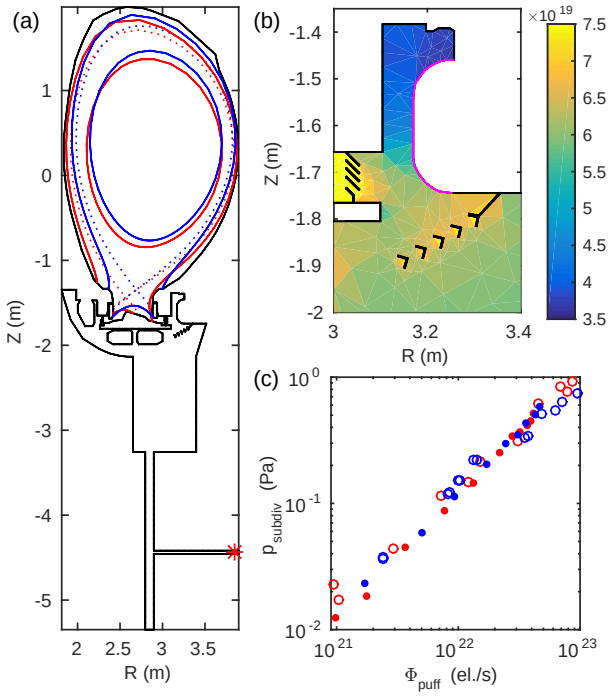

Figure 1: *(a) The simulation geometry. (b) The D_2 density (m^{-3}) near the cryopump surface (magenta line). (c) p_{subdiv} as a function of Φ_{puff} in experiment (open circles) and simulation (solid circles) and in HT (red) and VT (blue) configurations.*

Consider the experimentally measured p_{subdiv} as a function of Φ_{puff} (or equivalently Φ_{pump}), shown in figure 1c for both HT (red open circles) and VT (blue open circles) configurations. In the absence of neutral-neutral collisions, the pumped flux is the fraction of the surface-integrated one-way Maxwellian flux which sticks: $\Phi_{pump} = (1-\alpha_{pump}) \int n_{D2pump}.18.1\sqrt{T_{D2pump}}.dA_{pump}$, where n_{D2pump} and T_{D2pump} are the D_2 density (m^{-3}) and temperature (K) in front of the pump surface, and α_{pump} is the pump albedo. Our simulations show that the particle sources into the sub-divertor through the inner and outer throats remain equally balanced (within 20%) in VT for all values of Φ_{puff}, while in HT the flux through the outer throat always dominates (by at least a factor four). If this is also the case in experiment, then the D_2 density at the baratron will be a linear function of the density at the pump and $\Phi_{puff}/p_{subdiv} =$ constant, as seen to a good approximation in figure 1c (we assume that T_{D2pump} is set by the wall temperature so is independent of Φ_{puff}).

The action of the cryopump in the simulations is modelled by placing a pumping surface around the pump inlet (magenta line in figure 1b). Ideally, the albedo of this surface would be set by the cryopump speed measured in a gas of constant density. The ratio Φ_{puff}/p_{subdiv} would then be an output from the code. Unfortunately such a measurement was not available; only *in-situ*, effective pumping speeds have been published for the JET cryopump (e.g. [7]). Instead, a simulated albedo of $\alpha_{pump} = 0.92$ was set such that the experimental ratio of Φ_{puff}/p_{subdiv} was recovered, as shown by the solid circles in figure 1c. Although this methodology means that Φ_{puff}/p_{subdiv} is not an

output from the code, the absolute magnitude of Φ_{puff} for a given upstream density is. This is in contrast to versions of the code without the sub-divertor module, in which the EIRENE grid was cut off at the inner and outer divertor corners and pumping was modelled by placing surfaces with a prescribed albedo α_{pump} in those corners (e.g. [8]). The value used for α_{pump} was typically chosen such that the simulated puff required to reach a given upstream separatrix density was similar to that required in experiment; Φ_{puff} cannot then be considered an output from the code.

Simulation results

Plasma quantities calculated by EDGE2D-EIRENE simulations without the subdivertor module have been compared to this experiment previously in [5]. Plasma quantities are minimally affected by the inclusion of the subdivertor module because the recycling target flux dominates over Φ_{puff} [9]. We therefore focus on a comparison of Φ_{puff}. Figure 2 plots Φ_{puff} as a function of the outer mid-plane separatrix electron density $n_{\text{e,sep,OMP}}$, in HT (red) and VT (blue) configurations, and in experiment (open circles) and simulation (solid circles). It is assumed here the experimentally measured line-averaged edge density is twice $n_{\text{e,sep,OMP}}$ [10]. The puff required to achieve a given density was a factor 2-3 larger in VT than in HT. Simulation results are within a factor $\sim$2 of experiment, with a tendency to overestimate Φ_{puff} at low density and underestimate Φ_{puff} at high density. Furthermore, the simulations successfully recover the higher Φ_{puff} in VT.

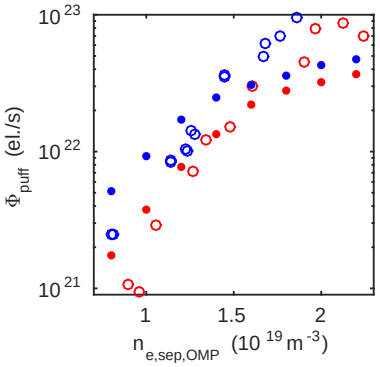

Figure 2: Φ_{puff} *as a function of* $n_{\text{e,sep,OMP}}$ *in experiment (open circles) and simulation (solid circles) and in HT (red) and VT (blue) configurations.*

To understand why a higher Φ_{puff} is required in VT than in HT, we focus on a low density simulation with $n_{\text{e,sep,OMP}} = 8.5 \times 10^{18}$ m^{-3}, for which a good agreement between experimental and simulation target data was found. At higher densities the argeement with experiment worsens [5], so that the reason for higher pumping in VT can be less trusted. Figure 3 shows the core penetration efficiency, defined as the percentage of a target's recycling flux which ionises inside the separatrix, from the inner and outer targets and for HT and VT configurations. From both targets, the fraction of neutrals penetrating the separatrix and contributing to $n_{\text{e,sep,OMP}}$ is significantly higher in HT than in VT. Thus, an increased target recycling flux (two times higher in our simulations) is required to achieve $n_{\text{e,sep,OMP}} = 8.5 \times 10^{18}$ m^{-3} in VT, which in turn requires a higher Φ_{puff}. Note that this effect is self reinforcing since a higher target recycling flux leads to a higher divertor density which leads to a decreased core penetration.

We hypothesise the increased penetration in HT to be caused by a combination of two factors: the x-point is 1.9 times closer to the inner target in HT than in VT, and neutrals preferentially recycle near the separatrix in VT compared to HT. Disentanglement of the relative role of these two factors is future work, however the fact that the difference between HT and VT penetration efficiencies is largest at the inner target suggests that the location of the x-point plays an important role in setting Φ_{puff} at this density.

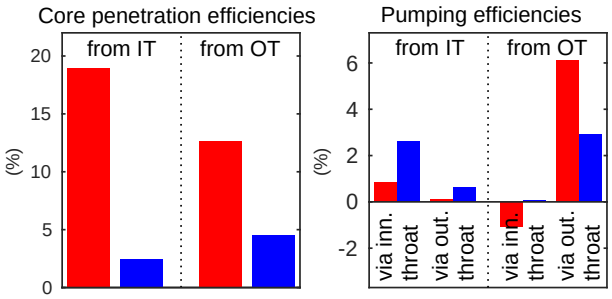

Figure 3: *Simulated core penetration and pumping efficiencies HT (red) and VT (blue) for a low density case, from outer and inner targets. Pumping efficiencies are further divided into fluxes via the inner and outer divertor throats.*

Also shown in figure 3 are the simulated pumping efficiencies, defined as the percentage of a particular target's recycling flux which is pumped. These have been further divided by the throat via which the neutrals flow before being pumped. The pumping in VT is seen to be more balanced compared to HT, in which most of the pumped flux is from the outer target, via the outer throat into which the outer target is angled. However, the *total* pumping efficiencies, i.e. the total recycling flux from both targets divided by the total pumped flux, are very similar in HT and VT (3.3% in HT compared to 3.2% in VT). The higher Φ_{puff} in VT at this density cannot therefore be attributed to an improved pumping efficiency. Furthermore, at this $n_{\text{e,sep,OMP}}$ (unusually for this dataset), both VT and HT configurations were actually puffed entirely from the top of the machine, in experiment and simulation. Direct pumping of the puff can therefore be ruled out as a reason for the higher Φ_{puff} in VT, as previously speculated [5]. Rather, at this low density it is the increased core penetration in HT that is the dominant cause of an increased Φ_{puff} in VT.

This work has been carried out within the framework of the EUROfusion Consortium and has received funding from the Euratom research and training programme 2014-2018 under grant agreement No 633053. The views and opinions expressed herein do not necessarily reflect those of the European Commission.

References

[1] A. S. Kukushkin *et al.*, Fusion Eng. Des. **86**, 2865 (2011)
[2] R. Simonini *et al.*, Contrib. Plasma Phys. **34**, 368 (1994)
[3] D. Reiter *et al.*, J. Nucl. Mater. **196-198**, 80 (1992)
[4] S. Wiesen *et al.*, ITC project report 2005/6, http://www.eirene.de/e2deir_report_30jun06.pdf
[5] M. Groth *et al.*, J. Nucl. Mater., doi:10.1016/j.jnucmat.2014.12.030 (2014)
[6] S. Brezinsek *et al.*, Nucl. Fusion **53**, 083023 (2013)
[7] V. Philipps *et al.*, J. Nucl. Mater. **390-391**, 478 (2009)
[8] D. Moulton *et al.*, J. Nucl. Mater. **415**, S509 (2011)
[9] A. V. Chankin *et al.*, Plasma Phys. Contr. F. **48**, 839 (2006)
[10] M. Groth *et al.*, J. Nucl. Mater. **438**, S175 (2013)